Effect of organic additives on the mitigation of volatility of 1-nitro-3,3′-dinitroazetidine (TNAZ): Next generation powerful melt cast able high energy material

M.B. Talawar [a,*], Alok Singh [b], N.H. Naik [a], B.G. Polke [a], G.M. Gore [a], S.N. Asthana [a], B.R. Gandhe [a]

[a] *High Energy Materials Research Laboratory, Pune 411 021, India*
[b] *National Chemical Laboratory, Pune 411 008, India*

Abstract

1-Nitro-3,3′-dinitroazetidine (TNAZ) was synthesized based on the lines of reported method. Thermolysis studies on synthesized and characterized TNAZ using differential scanning calorimetry (DSC) and hyphenated TG-FT-IR techniques were undertaken to generate data on decomposition pattern. FT-IR of decomposition products of TNAZ revealed the evolution of oxides of nitrogen and HCN containing species suggesting the cleavage of $C/N–NO_2$ bond accompanied with the collapse of ring structure. The effect of incorporation of 15% additives namely, 3-amino-1,2,4-triazole (AT), 3,5-diamino-1,2,4-triazole (DAT), carbohydrazide (CHZ), 5,7-dinitrobenzofuroxan (DNBF), bis (2,2-dinitropropyl) succinate (BNPS), triaminoguanidinium nitrate (TAGN), 2,4,6-trinitrobenzoic acid (TNBA) and nitroguanidine (NQ) on the volatility of TNAZ was investigated by undertaking thermogravimetric analysis. The TG pattern brings out the potential of BNPS and TAGN as additives to mitigate the volatility of TNAZ. The influence of additives on thermal decomposition of pattern of TNAZ was also investigated by DSC. The DSC results indicated that the additives did not have appreciable effect on the melting point of TNAZ. Scanning electron microscopic (SEM) studies were carried out to investigate the effect of additives on morphology of TNAZ. This paper also discusses the possible mechanism involved in between the TNAZ and TAGN and BNPS. It appears that the formation of charge transfer complex formation between the TNAZ and TAGN/BNPS. The effect of addition of high explosives such as CL-20, HMX and RDX on thermo-physical characteristics of TNAZ is also reported in this paper.
© 2005 Elsevier B.V. All rights reserved.

Keywords: Trinitroazetidine (TNAZ); Melt castable explosive; Synthesis; Thermolysis; Morphological structure; Volatility behavior

1. Introduction

Strained polynitro cyclic compounds are among the fast emerging powerful high energy materials (HEMs) with low vulnerability. Polynitro bicyclo octane [1], polynitro cubanes [2], polynitro polycyclododecane [3] and variety of polynitro-cylicpolyaza nitramines [4–6] belong to this class. Such materials may find application in advanced propellant and explosive formulations. The azetidines particularly, 1,3,3-trinitroazetidine (TNAZ) [7–13] having strained four member heterocyclic ring have made foray in the area of melt castable explosive since 1990s.

TNAZ offers a combination of moderately low melting point (101 °C) and good thermal stability (>180 °C). Its attractive features compared to the today's most sought after melt castable explosive, 2,4,6-trinitrotoluene (TNT) are superior density (1.89 g/cm³) and velocity of detonation (>8500 m/s). One of the major drawbacks of TNAZ is its poor yield during synthesis [14–19]. The efforts are on all over the globe towards developing economically viable method for TNAZ synthesis. Various methods of synthesis of TNAZ have been reported by different schools.

The thermal behavior of TNAZ is investigated by various researchers [7–13] and the thermodynamic parameters of the melting process as well as kinetic parameters of the exothermic decompositions of TNAZ in molten/gas phase have also been reported. ATK Thiokol propulsion, USA, has been actively involved [20] with the development of melt/pour explosive

formulations based on TNAZ. However, major problem encountered during practical application of TNAZ is its volatility. Attempts are on to address this problem by lowering the melt temperature of TNAZ by adding additives in optimized quantities.

As TNAZ is gaining importance with the passage of time, generation of data on this fascinating compound is of great relevance. Accordingly, TNAZ was synthesized by the authors in the laboratory and characterized by IR, ^{1}H NMR and energy dispersive analysis of X-rays (EDAX) as well as subjected to thermal studies including hyphenated TG-FT-IR. Further, in view of the scanty reports [20] available on compounds capable of overcoming the volatility problems associated with TNAZ for practical applications, effect of incorporation of organic additives was also investigated. Heterocycles, viz., 3-aminotriazole (AT), 3,5-diaminotriazole (DAT), 5,7-dinitrobenzofuroxan (DNBF), and aromatic compounds like 2,4,6-trinitrobenzoic acid (TNB), as well as non-aromatic compounds such as bis dinitropropyl succinate (BNPS), triaminoguanidinium nitrate (TAGN), nitroguanidine (NQ), carbohydrazide (CHZ), hexahydro-1,3,5-trinitro-1,3,5-triazine (RDX), octahydro-1,3,5,7-tetranitro-1,3,5,7-tetazocine (HMX) and 2,4,6,8,10,12-hexanitrohexaaza isowurtzitane (CL-20) were selected in combination with TNAZ on the lines of work undertaken by Thiokol. SEM of additive incorporated TNAZ was undertaken to assess the effect on the morphological features.

2. Experimental

2.1. Materials and methods

The TNAZ was synthesized (Scheme 1) on the lines of the reported method [21,22]. The additives such as BNPS, RDX, HMX, CL-20, NQ, DNBF, DAT and AT were synthesized based on the lines of reported literature methods. The starting materials of AR grade, used for the synthesis of TNAZ, were purchased from the trade (Merk) and employed as such without further purification. The Fourier transform infrared (FT-IR) spectrum of the synthesized product was determined in KBr matrix on a Perkin-Elmer1600 FT-IR spectrophotometer. Proton NMR spectrum was recorded on Varian 300 MHz spectrometer with tetra methyl silane as an internal standard. TG-FT-IR of the product was undertaken on simultaneous thermo gravimetry—differential thermal analyzer (TG/SDTA-Mettler Toledo 8551) in conjunction with FT-IR of Bruker make (Model-55). The impact sensitivity test was conducted using a set up similar to that used in Naval Ordnance Laboratory (NOL), USA. Test specimens (30–35 mg of powder) were kept between two hardened stainless steel anvils and a 3 kg drop weight was allowed to fall freely from different heights. Both open and aluminum foil encapsulated specimens were used for evaluation. Ten tests were conducted for each compound. The results are reported in terms of height for 50% probability of explosion ($h_{50\%}$) of the sample. The friction test was also conducted in a test set up similar to the one employed by NOL. The sample was kept between a fixed corrugated (rough) and a movable stainless steel plate. Pulling of the movable plate at varying lever loads subjected sample to friction stimuli. The sample size and the procedure was same as followed for impact testing.

The TGA of additives incorporated TNAZ was also carried out on same setup at the heating rate of $10\,°C/min$. The DSC of TNAZ and its admixture with additives was performed on Perkin-Elmer-7 system at a heating rate of $10\,°C/min$ in nitrogen atmosphere. The DSC was undertaken on the precisely weighed samples amounting to ~1 mg. The SEM of the samples was recorded using Instrument of Philips XL-30 model. The energy of electron beam used for impinging on the samples was of the order of 5 kV.

3. Results and discussions

3.1. Synthesis and characterization

The intermediate compounds (Scheme 1) such as 1,3-dichloro-2-(tetrahydropyranyl) propane, 1,3-dibromo-2-(hydropyranyl) propane, 1-(p-tosyl)-3-(pyranyl) azitidine, 1-toluene
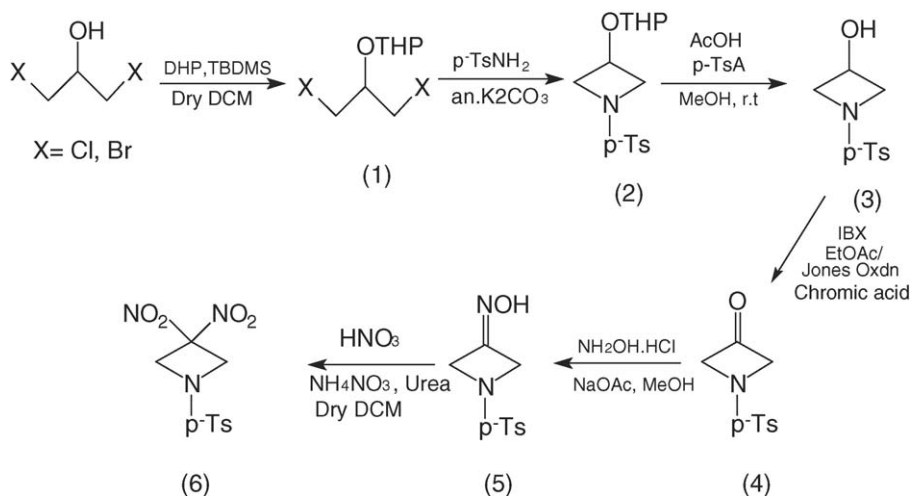
Scheme 1. Synthesis of TNAZ. (i) DHP: dihydropyran; (ii) DCM: dichloromethane; (iii) THP: tetrahydropyranyl; (iv) p-TsNH₂: p-toluene sulphonamide; (v) TBDMS: tert-butyldimethylsilyl ether; (vi) IBX: 2-iodoxybenzoic acid; (vii) p-TsA: p-toluene sulphonic acid; (viii) AcOH: acetic acid.

sulphonyl azetidine-3-ol, 1-(*p*-toluene sulfonyl) azetidine-3-one and 3-oximido-1-(*p*-toluene sulfonyl) azetidine were synthesized based on the line of reported methods [21,22] and were characterized by spectral data before utilizing for the synthesis of the final product:

(a) 1,3-Dichloro-2-(tetrahydropyranyl) propane (**1**). Boiling point: 105–106 °C; ^{1}H NMR (CDCl$_3$): δ 1.4 (m, 6H, 3× CH$_2$), 3.75 (m, 8H).

(b) 1-(*p*-Tosyl)-3-(tetrahydro pyranyl) azetidine (**2**). Melting point: 60–62 °C; ^{1}H NMR (CDCl$_3$): δ 1.5 (m, 6H, 3× CH$_2$), 2.45 (S, 3H, CH$_3$), 3.65 (m, 4H, 2× CH$_2$), 4.0 (t, 2H, CH$_2$), 4.35 (m, 1H, CH), 4.5 (t, 1H, CH), 7.6 (d, 2H, 2× CH), 7.75 (d, 2H, 2× CH).

(c) 1-(*p*-Toluene sulfonyl) azetidine-3-ol (**3**). Melting point: 103–104 °C; ^{1}H NMR (CDCl$_3$): δ 2.5 (s, 3H, CH$_3$), 2.6 (br, s, OH), 3.6 (t, 2H, CH$_2$), 4.05 (t, 2H, CH$_2$), 4.5 (m, 1H, CH), 7.4 (d, 2H, 2× CH), 7.8 (d, 2H, 2× CH).

(d) 1-(*p*-Toluene sulfonyl) azetidine-3-one (**4**). Melting point: 146–147 °C; ^{1}H NMR (CDCl$_3$): δ 2.45 (s, 3H, CH$_3$), 4.65 (s, 4H, 2× CH$_2$), 7.4 (d, 2H, 2× CH), 7.8 (d, 2H, 2× CH).

(e) 3-Oximido-1-(*p*-toluene sulfonyl) azetidine (**5**). Melting point: 170–172 °C; ^{1}H NMR (CDCl$_3$): δ 2.44 (s, 3H, CH$_3$), 4.5 (d, 4H, 2× CH$_2$), 7.35 (d, 2H, 2× CH), 7.75 (d, 2H, 2× CH).

3.2. Spectral and thermolysis of TNAZ

The ^{1}H NMR data obtained for the precursors is in close agreement with the reported data [22]. The yield of TNAZ obtained during the present work was 30–35%. IR (cm^{-1}): 3036, 2970, 2910 (CH), 1594 (N–NO$_2$), 1540 (C–NO$_2$), 1426 (C–N), 1334, 1278, 1216, 1112, 1086, 908, 868, 840, 762, 712 (heterocyclic ring); ^{1}H NMR (δ): 5.19 (4H, s, 2× CH$_2$). EDAX of
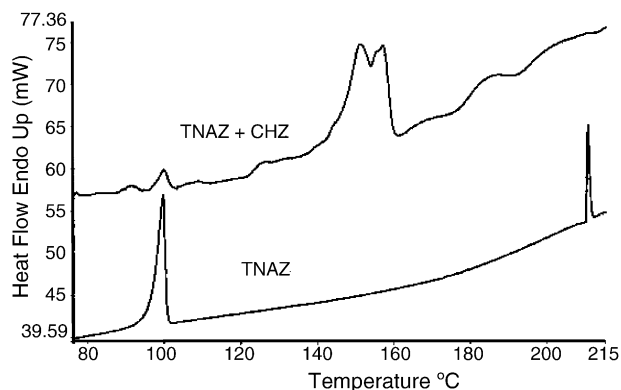

Fig. 1. DSC of TNAZ (100%) and TNAZ (85%) + CHZ (15%).

TNAZ gave nitrogen (29.27%) and oxygen (42%) content in close agreement with the theoretical values (nitrogen: 29.17%; oxygen: 42.3%). The DSC of TNAZ (Fig. 1) exhibited a sharp endotherm at 100 °C corresponding to its melting point (ΔH of 158.4 J/g). The endotherm was followed by exotherm with T_{max} at 214 °C (ΔH of 68.41 J/g). These results are in close agreement with the reported [18] values and bring out that its stability is intermediate to that of RDX and TNT. A minor exotherm was also observed at 194 °C (ΔH of 9.3 J/g).

In TGA, TNAZ recorded weight loss (Fig. 2) in the temperature range of 100–130 and 130–170 °C. The weight loss in the first step may be attributed to its volatilization whereas the evaporation of the compound accompanied with partial decomposition may be occurring during second step. Owing to the complexity of phenomenon due to interplay between evaporation and decomposition, the results are expected to be valid for a given experimental set up. The rapid rate of evaporation of TNAZ from the molten phase is of concern from safety and processing viewpoint.
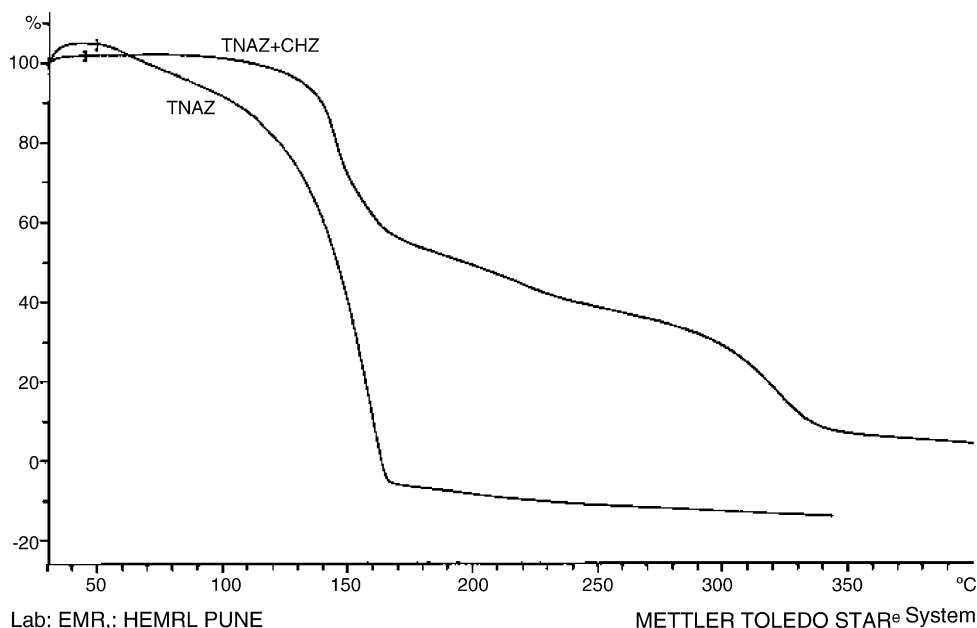

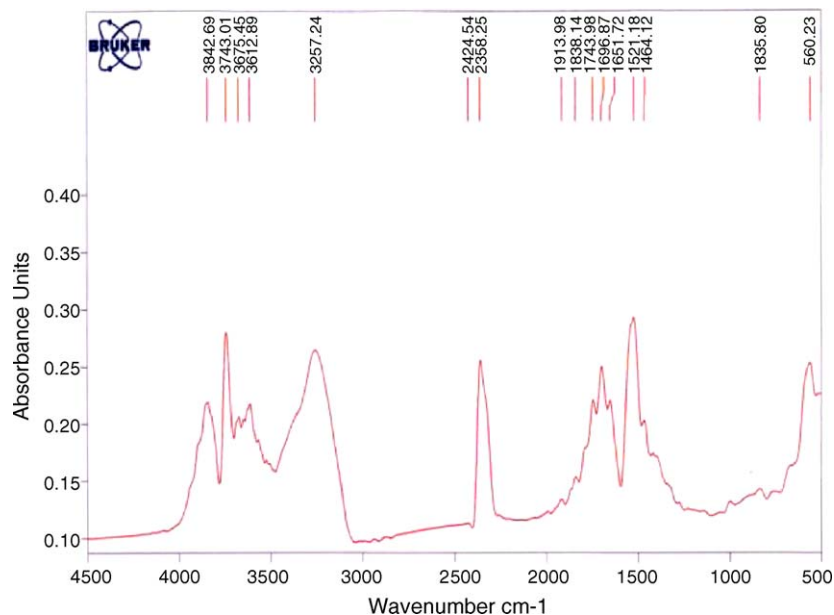Fig. 2. TG of TNAZ (100%), and the combination of TNAZ (85%) + CHZ (15%).

Fig. 3. TG-FT-IR of TNAZ.

The FT-IR of gaseous decomposition products (Fig. 3) of TNAZ evolved during TG revealed the presence of NO ($1521 \, cm^{-1}$), NO_2 ($1651 \, cm^{-1}$), H_2O (3842, 3743 and $3675 \, cm^{-1}$), HCN (2358, $1464 \, cm^{-1}$), CO ($2424 \, cm^{-1}$). The oxides of nitrogen may result from the cleavage of the both N–NO_2 and C–NO_2 linkages, where as evolution of species like HCN may be an outcome of the cleavage of ring structure. The results obtained are in line with the data reported by other researchers.

Various researchers identified 1-nitroso-3,3-dinitroazetidine (NDNAZ) as the stable intermediate of thermal decomposition of TNAZ in condensed phase [24]. The SCF-MO-AM1 calculations [23] suggest the homolysis of N–NO_2 bond as the primary step of thermolysis of secondary nitramines in a condensed phase [19]. The strained structure of TNAZ is expected to favor the collapse of the heterocyclic ring.

3.3. Sensitivity properties of TNAZ

The sensitivity test results brought out that TNAZ is impact insensitive up to 47 cm ($h_{50\%}$ explosion) and it is friction insensitive up to load of >36 kg. These trends suggest its overall low vulnerability to mechanical stimuli compared to that of other nitramine explosives such as RDX and HMX ($h_{50\%}$ friction insensitive up to 16 and 19 kg, respectively).
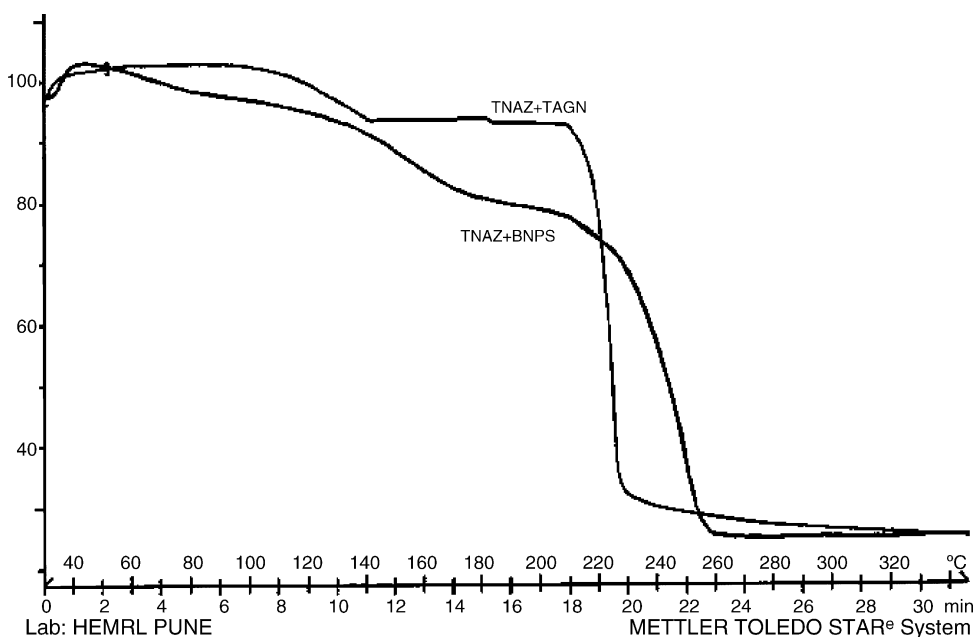

Fig. 4. TG of TNAZ (85%) + TAGN (15%) and TNAZ (85%) + BNPS (15%).
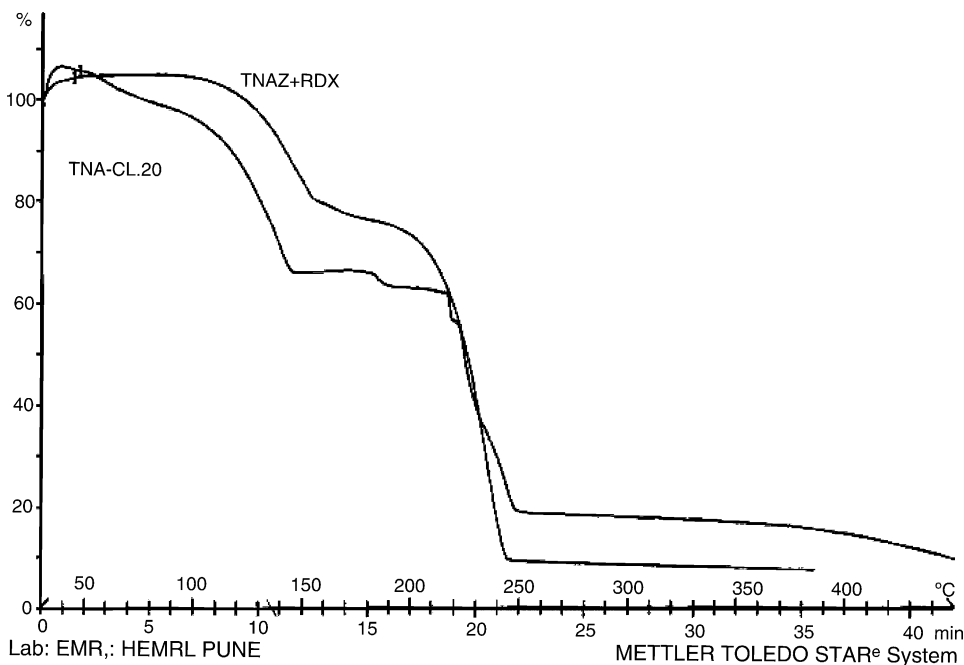
Fig. 5. TG of TNAZ (85%) + RDX (15%) and TNAZ (85%) + CL-20 (15%).

3.4. Additives incorporated TNAZ

3.4.1. Thermogravimeric analysis

In TG (Figs. 2 and 4–8), all the additives brought down the extent of weight loss during initial stages, i.e. up to 130 °C except NQ (Fig. 6). A remarkable decrease in the weight loss up to 180 °C was exhibited in BNPS (Fig. 4) and TAGN (Fig. 4) incorporated TNAZ. Among RDX (Fig. 5), HMX (Fig. 6) and CL-20 (Fig. 5) incorporated TNAZ mix, HMX containing TNAZ exhibited relatively less weight loss in the initial stage (Table 1).

3.4.2. Differential scanning calorimeter

Additives did not have appreciable effect on the endotherm due to melting of TNAZ (Figs. 1 and 9–13). Incorporation of AT drastically brought down the T_m, of the following exotherm, whereas DNBF (Fig. 9), TAGN (Fig. 12) and DAT (Fig. 13) brought it down to a lesser extent. The incorporation of NQ
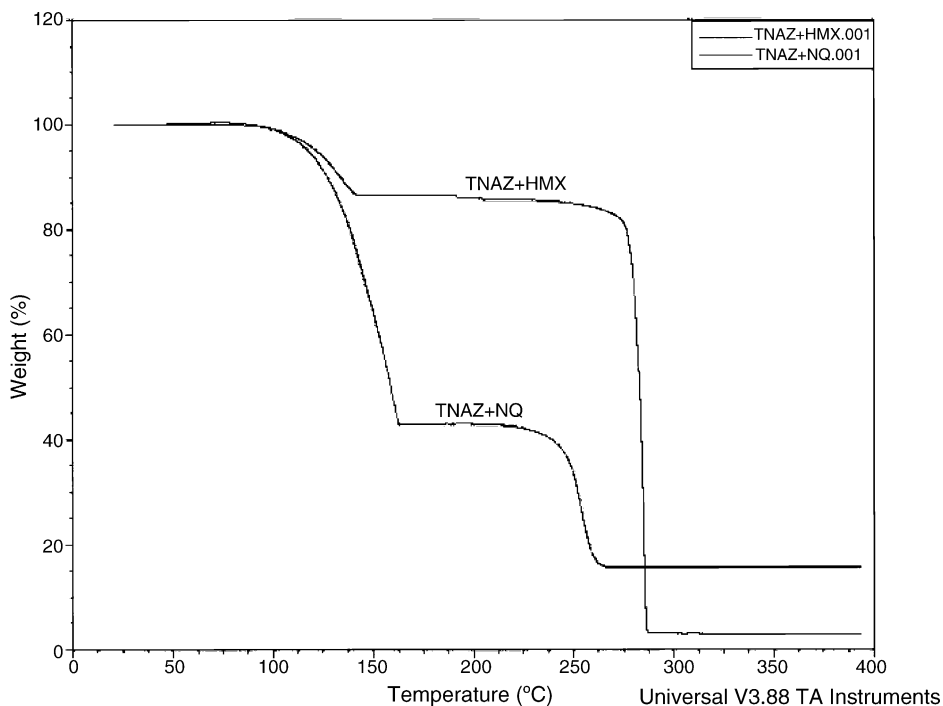
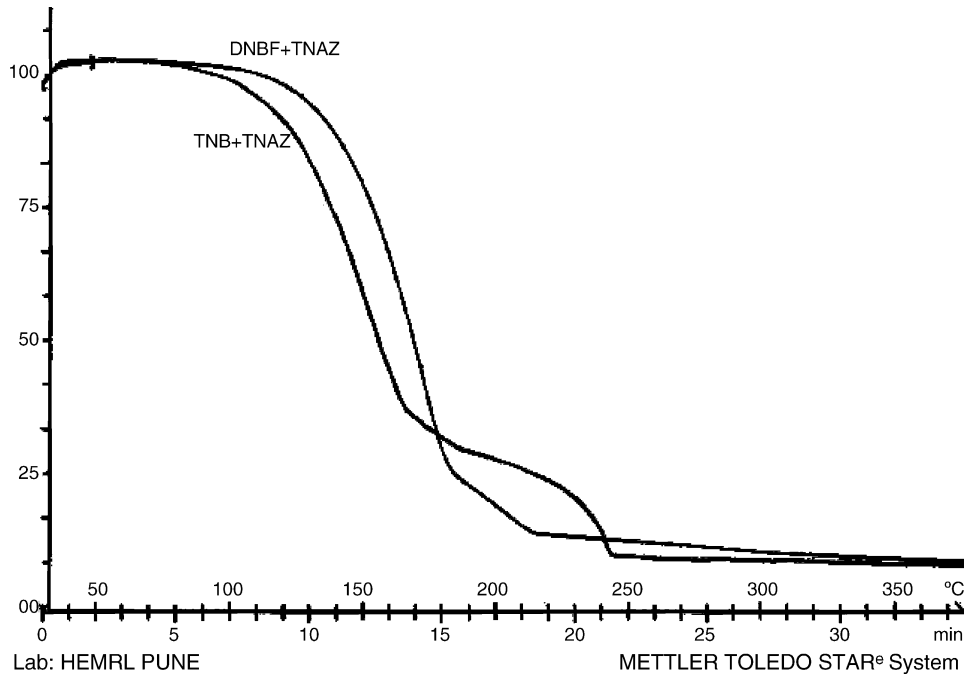Fig. 6. TG of TNAZ (85%) + HMX (15%) and TNAZ (85%) + NQ (15%).

Fig. 7. TG of TNAZ (85%) + DNBF (15%) and TNAZ (85%) + TNB (15%).

(Fig. 11), BNPS (Fig. 12) and TNB (Fig. 9) resulted in increase in T_m. The effect was more pronounced with BNPS (Fig. 12). Surprisingly CHZ (Fig. 1) incorporated TNAZ underwent endothermic decomposition. RDX/CL-20 (Fig. 10)/HMX (Fig. 11) incorporated TNAZ exhibited exothermic decomposition with T_{max} close to that for the former (Table 1).

3.4.3. Scanning electron microscopy

The morphological nature of TNAZ alone and TNAZ in combination with other organic additives is given in Figs. 14–25.

In SEM, TNAZ revealed rod and flake morphology (Fig. 14). The additives such as BNPS (Fig. 16), TAGN (Fig. 17), NQ (Fig. 21), TNB (Fig. 23) and DAT (Fig. 24) did not have much effect on the morphology of TNAZ (Fig. 14). Incorporation of CHZ (Fig. 15) resulted in formation of agglomerate where as DNBF (Fig. 22), TNB (Fig. 23), and AT (Fig. 25) rendered it amorphous. RDX (Fig. 18) incorporated TNAZ revealed crystal structure of both RDX and TNAZ where as addition of HMX (Fig. 20) led to change in the morphology to amorphous.
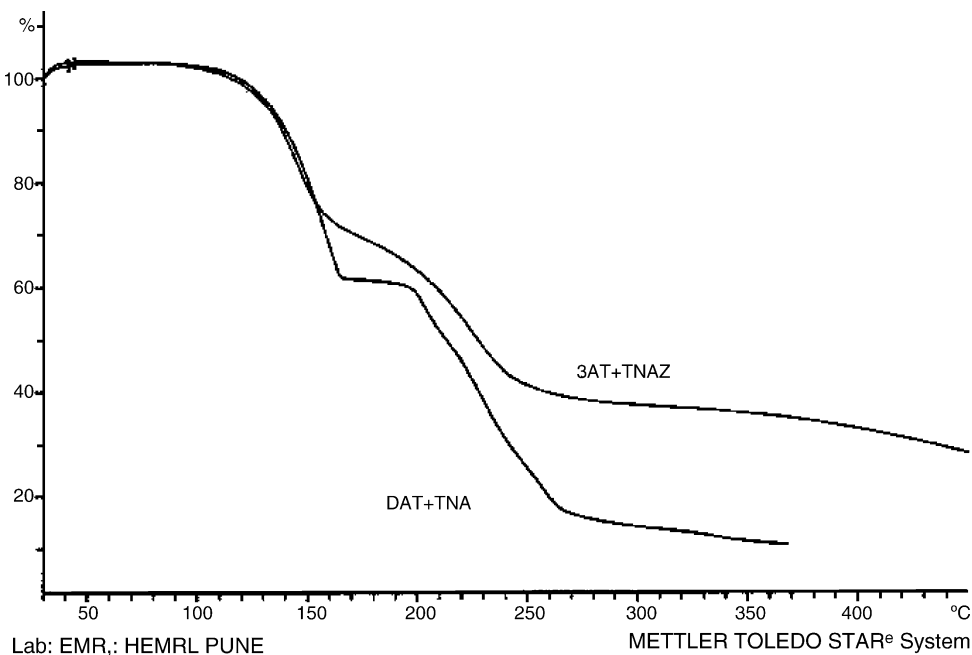

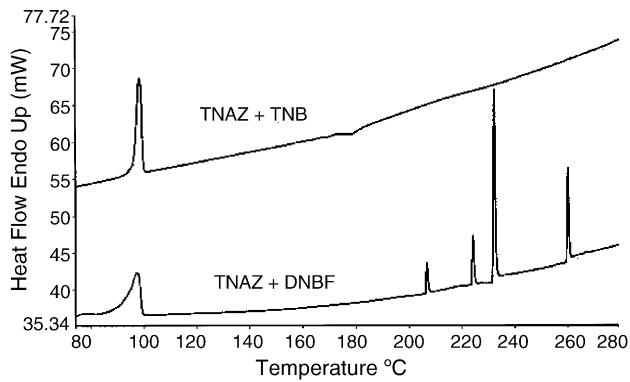Fig. 8. TG of TNAZ (85%) + DAT (15%) and TNAZ (85%) + 3-AT (15%).

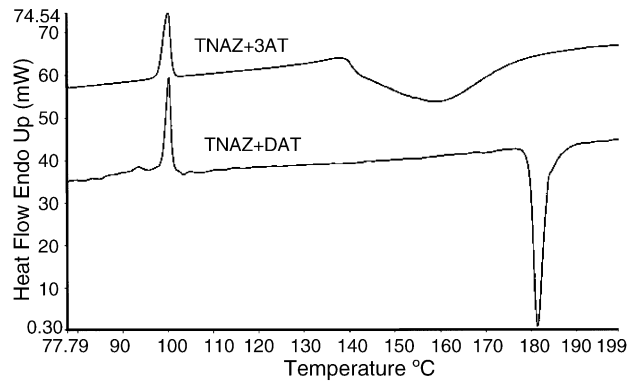Fig. 9. DSC of TNAZ (85%) + DNBF (15%) and TNAZ (85%) + TNB (15%).
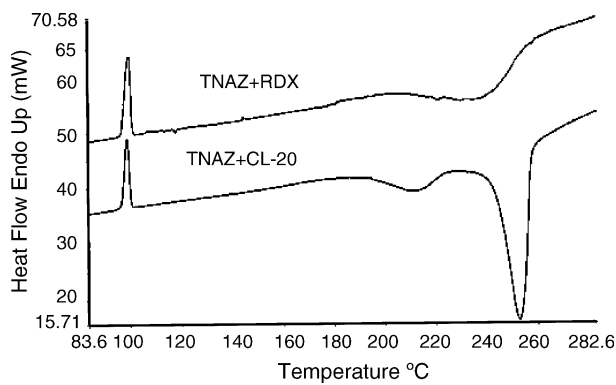

Fig. 10. DSC of TNAZ (85%) + RDX (15%) and TNAZ (85%) + CL-20 (15%).
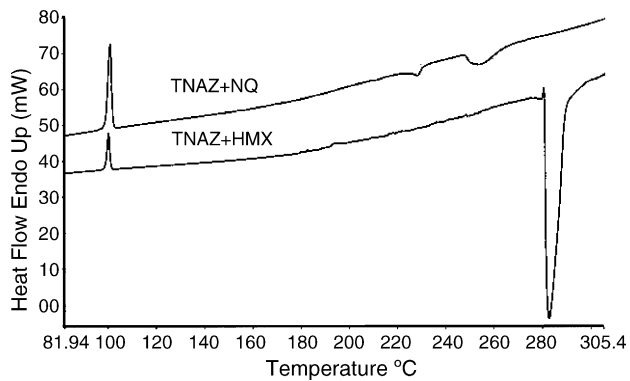

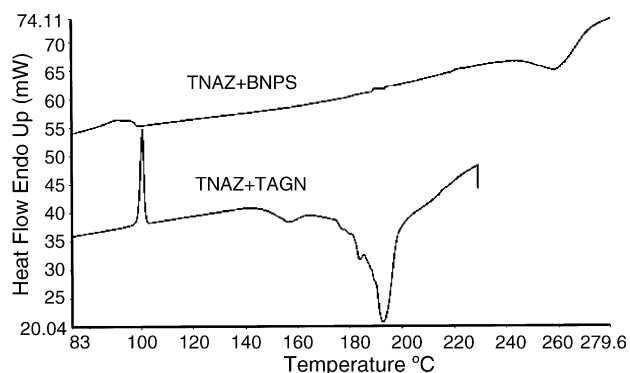Fig. 11. DSC of TNAZ (85%) + HMX (15%) and TNAZ (85%) + NQ (15%).

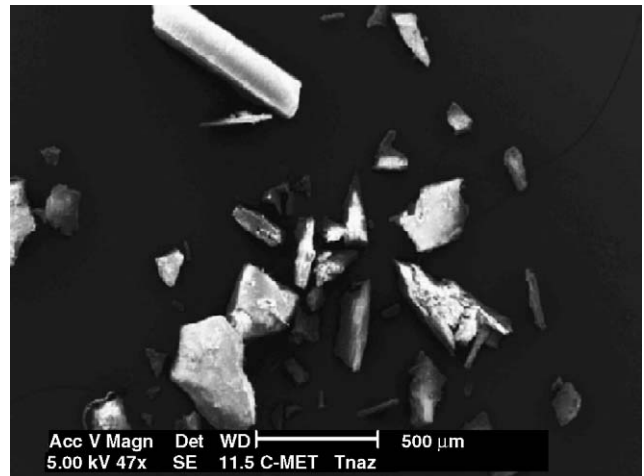Fig. 12. DSC of TNAZ (85%) + TAGN (15%) and TNAZ (85%) + BNPS (15%).

Fig. 13. DSC of TNAZ (85%) + DAT (15%) and TNAZ (85%) + 3-AT (15%).
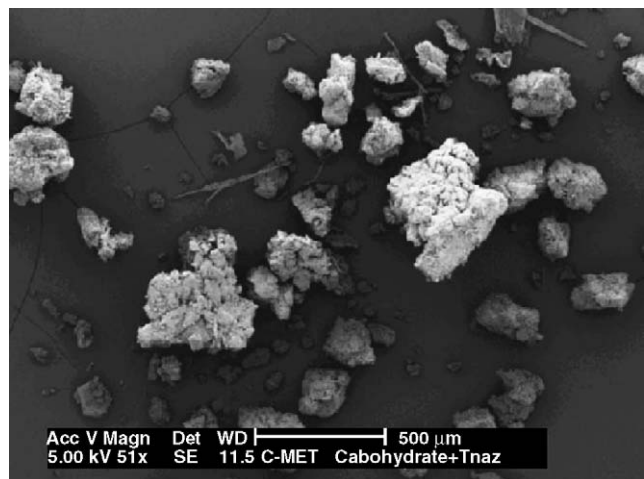

Fig. 14. SEM of TNAZ.

Fig. 15. SEM of TNAZ (85%) + CHZ (15%).

4. Mechanistic role of TAGN and BNPS in reducing the volatility of TNAZ

The volatility of TNAZ may be mainly due to weak intermolecular interactions (weak Vanderwaals forces). It may be an outcome of the possibility of hindrance to the approach of the negatively charged oxygen of the NO_2 of a given TNAZ

Table 1
TG results of TNAZ alone and mixed with other additives

| Samples	TG data		DSC data	
	% Weight loss (Temperature region, °C)	E_a (kJ/mol)	First endo (°C)	Second exo (°C)
TNAZ	27 (98–130)	54	100.76	194
	72 (133–180)	75		214
TNAZ + NQ	43 (100–165)	80	100.83	228
	15 (225–262)	133		254
TNAZ + BNPS	7 (100–132)	34.16	97	258
	17 (133–197)	102		
	66 (198–270)	155		
TNAZ + TAGN	5 (100–145)	99.3	100.43	192
	72 (180–235)	400		
TNAZ + CHZ	6 (100–130)	28.46	98	–
	42 (131–180)	402		
	11 (181–235)	6	148	
	32 (236–345)	90	188	
TNAZ + 3,5-DAT	41 (100–170)	83.69	100.1	181.37
	46.5 (166–280)	43.79		
TNAZ + DNBF	10 (100–135)	81	97.47	206
	70 (131–182)	66		
	11 (182–230)	32		
TNAZ + TNB	7 (100–130)	87	100.3	237.50
	64 (131–190)	91		
	21 (191–240)	16		
TNAZ + 3-AT	7 (100–130)	80	99.90	159.70
	28 (131–182)	233		
	31 (183–262)	90		
TNAZ + CL-20	32.63 (100–155)	66.19	99.63	252
	47.76 (175–266)	180		
TNAZ + RDX	28 (100–180)	81	100.23	238
	66 (181–250)	149.67		
TNAZ + HMX	14 (100–153)	84.23	100	282
	84 (154–324)	140.6		
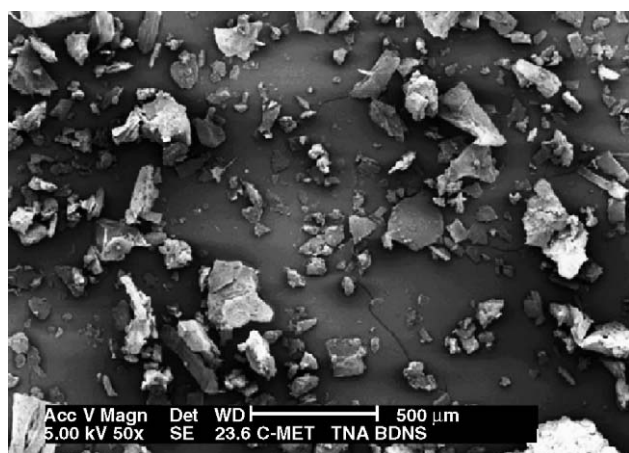
Fig. 16. SEM of TNAZ (85%) + BNPS (15%).
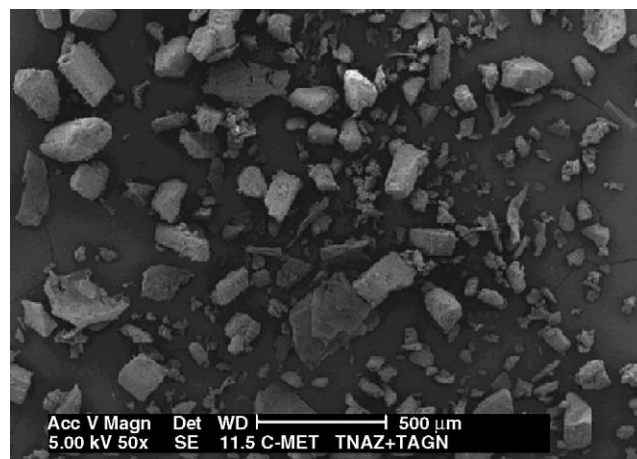
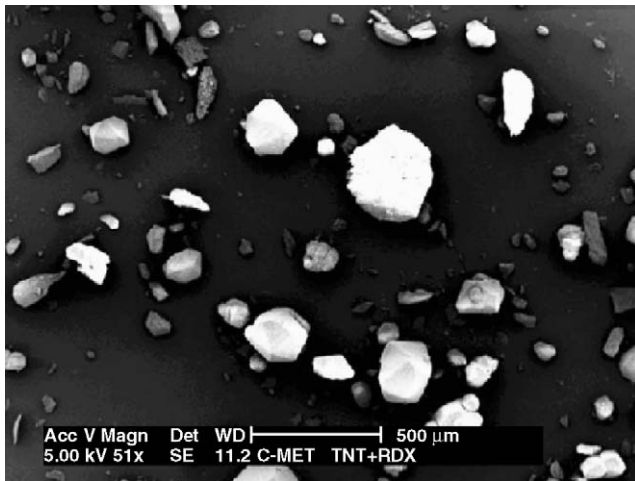Fig. 17. SEM of TNAZ (85%) + TAGN (15%).

Fig. 18. SEM of TNAZ (85%) + RDX (15%).
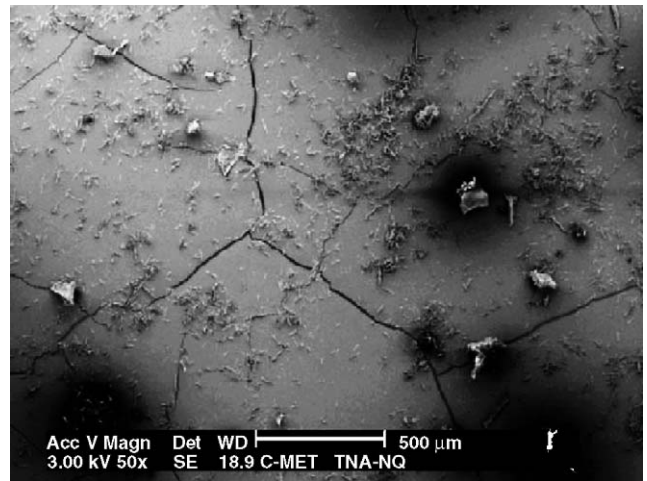

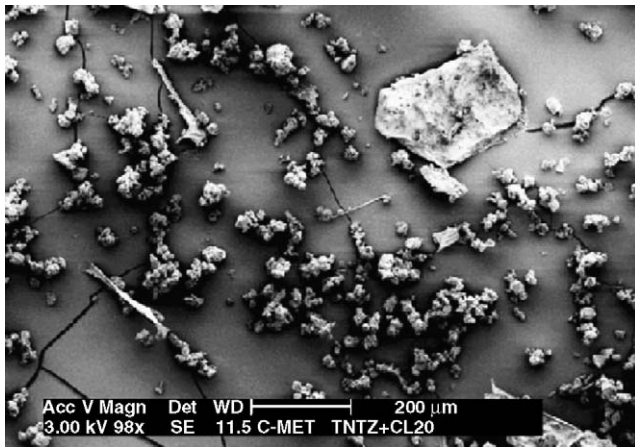Fig. 21. SEM of TNAZ (85%) + NQ (15%).

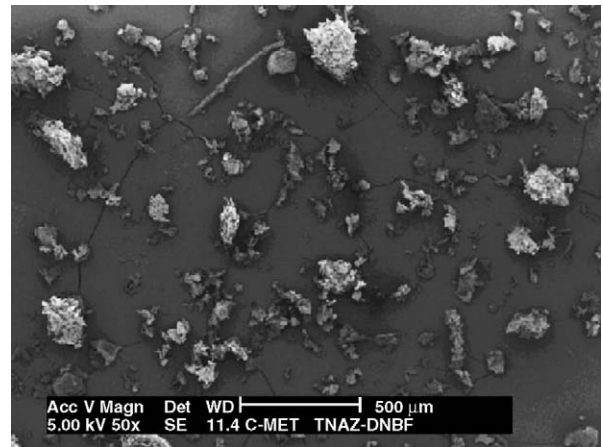Fig. 19. SEM of TNAZ (85%) + CL-20 (15%).
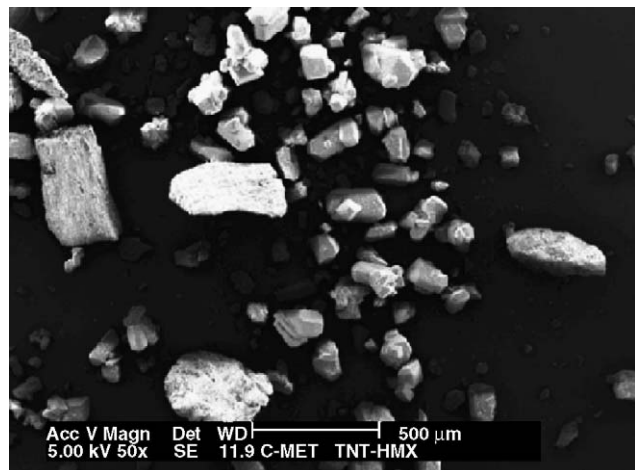

Fig. 22. SEM of TNAZ (85%) + DNBF (15%).
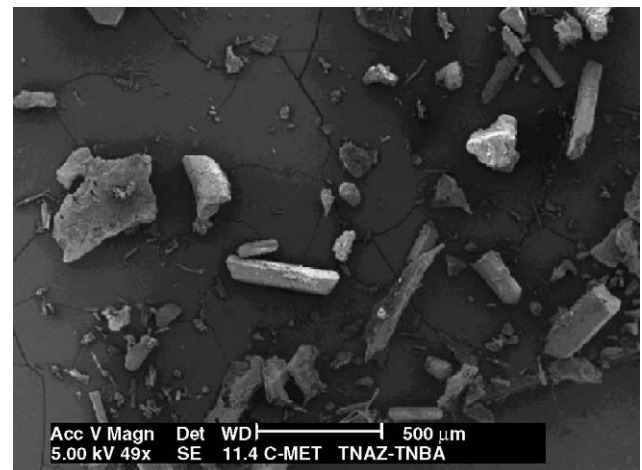

Fig. 20. SEM of TNAZ (85%) + HMX (15%).

Fig. 23. SEM of TNAZ (85%) + TNB (15%).

Table 2
IR data of TNAZ and additive-TNAZ at 100 °C

| TNAZ	TAGN	TNAZ + TAGN	BNPS	TNAZ + BNPS
3036	3348, 3226	3030 (−ve shift w.r.t. both)	3030	(−ve shift w.r.t. TNAZ)
2972, 2910	2798	2982 (+ve shift w.r.t TNAZ), 2900 (w), 2798 (w)	2894, 2984	2976 (−ve shift), 2902 (−ve shift)
2356	2452, 2354	–	2360	2350
1756	1686	1760 (+ve shift w.r.t. both)	1760	1760 (merged with BNPS)
1596	1570	1568 (−ve shift w.r.t. TNAZ)	1570	1570, 1596, 1540
1540		1404 (−ve shift w.r.t. TNAZ)	1454	1454 (missing)
1426		1328 (no significant change)	1404	1404 (negative shift w.r.t. TNAZ)
1332	1326, 1134	1282 (−ve shift w.r.t. TNAZ)	1326	1332 (no change)
1276	1050	1208, 1134, 1026 (−ve shift w.r.t. both)	1290	1278 (no change)
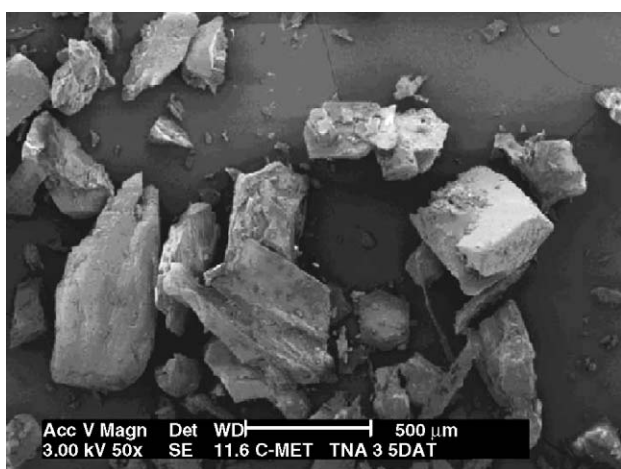
Fig. 24. SEM of TNAZ (85%) + DAT (15%).

molecule to the acidic methylene proton of the neighboring TNAZ molecule due to the presence of bulky NO$_2$ groups adjacent to latter (methylene proton). Moreover, there is possibility of effective intramolecular polar interactions between negatively charged oxygen of the NO$_2$ and acidic methylene protons.

Remarkable influence of TAGN in reducing the volatility of TNAZ observed during thermo gravimetric studies may be an outcome of the involvement of its lone pair of electrons on amino
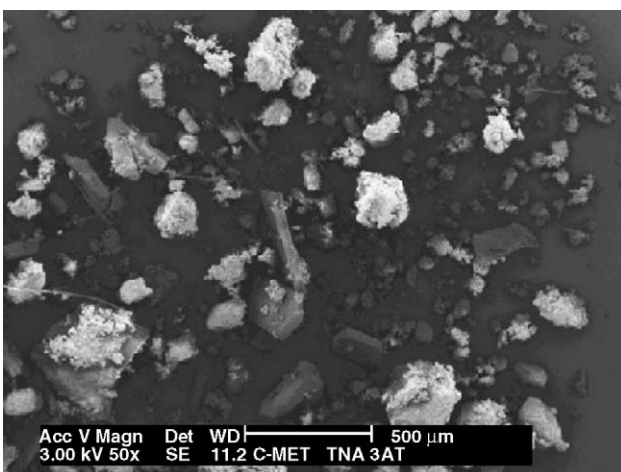

Fig. 25. SEM of TNAZ (85%) + 3-AT (15%).

group with the positively charged nitrogen of NO$_2$ group of TNAZ. Such interactions between compounds containing NO$_2$ and amino groups are reported in literatures [25,26] and the interaction of the NO$_3^-$ of the TAGN with the methylene group of the TNAZ.

In order to generate evidences, UV and IR spectra of the TNAZ and TAGN were determined at both ambient temperature and 100 °C. The IR of the individual compounds did not reveal appreciable charge with respect to temperature. However, TAGN added TNAZ showed negative shift in the IR band corresponding to TAGN (3226 → 3030 cm^{-1}) and positive shift in CH$_2$ frequencies of TNAZ (2972 → 2982 cm^{-1}) at 100 °C. This finding suggests formation of charge transfer complex. Supporting evidences were also provided by UV spectral data. The addition of TAGN to TNAZ (284, 303 and 310 nm) leads to shift in n → π* transitions of NO$_3^-$ to lower (268 and 282 nm) absorption. The results obtained in the present investigation calls for further in-depth study to establish the mechanistic role of TAGN in reducing the volatility of TNAZ.

The role of BNPS in mitigating the volatilization of TNAZ appears to be complex one as the IR of BNPS added TNAZ did not exhibit much change with respect to that of individual compounds. However, IR stretching frequency of 1290 cm^{-1} due to C–O–C of reduced to 1278 cm^{-1}. This suggests the probable formation of charge transfer complex between oxygen of C–O–C group and methylene/nitrogen of NO$_2$ group of TNAZ. The IR spectrum of BNPS added TNAZ sample also showed the negative shift from 1596 to 1570 cm^{-1}. This clearly indicates the involvement of TNAZ in charge transfer complexes formation (Table 2). The UV spectrum of BNPS added TNAZ sample showed the disappearance of n → π* transition at 270 nm (TNAZ) and 275 nm (BNPS). This gives an indirect hint of participation of nitro group of TNAZ with C–O–C group of BNPS and NO$_2$ group of TNAZ. Further in-depth studies need to be carried out to establish the mechanism or role of BNPS in reducing the volatility of TNAZ.

5. Conclusions

IR and EDAX pattern confirm the formation of the TNAZ during this work. The DSC pattern of TNAZ was in close agreement with that of reported by the other researchers. FT-IR of gas decomposition product suggests the cleavage of R–NO$_2$ bond accompanied with the rupture of the ring structure. The additives

did not have influence on melting process of TNAZ. However, BNPS and TAGN brought down the extent of overall volatility. DSC results suggest incompatibility of AT with TNAZ. Carbohydrazide appears to render overall decomposition process endothermic. The SEM studies brought that DNBF and AT render TNAZ amorphous, where as additives such as CHZ caused the agglomeration of TNAZ. The present investigation calls for the in-depth studies on the compatibility, performance and sensitivity aspects on the additive—TNAZ based compositions.

Acknowledgements

References

[1] G.A. Olah, P. Ramaiah, G.K. Surya Prakash, R. Gilardi, J. Org. Chem. 58 (1993) 763.

[2] P.E. Eaton, Angew. Chem. Int. Ed. 31 (1992) 1421; P.E. Eaton, J. Org. Chem. 53 (1988) 5353.

[3] L.A. Paquette, L.A. Fischer Engel, J. Org. Chem. 50 (1985) 2524.

[4] A.T. Nielson, in: G.A. Olah, D.R. Squires (Eds.), Chemistry of Energetic Materials, Academic Press, NewYork, 1991, p. 95.

[5] A.T. Nielson, R. Nissan, A.P. Chaffin, R.D. Gilardi, C. George, J. Org. Chem. 57 (1992) 6756.

[6] D. Chichra, H.G. Adolph, Synthesis (1983) 830; H.L. Ammon, R.D. Gilardi, S.K. Bhattacharjee, Acta Crytallogr. C39 (1983) 1680.

[7] Army SBIR Award (Phase I) No. A 96-013, U.S. Army Res. Office, Res., Triangle Park, NC, 1966. http://www.aro.ncren.net/Arowash/rt/a9620031.htm1.

[8] S. Borman, Chem. Eng. News 72 (1994) 18.

[9] G.A. Olah, D.R. Squire, Chemistry of Energetic Materials, Academic Press, San Diego, 1991.

[10] R.I. Simpson, R.G. Garza, M.F. Foltz, D.I. Ornellas, P.A. Utriev, Characterization of TNAZ, Rep. UCRL-ID-119572, Lawrence Livermore Lab., 1994.

[11] Sanderson, Proceedings of the 27th International Annual Conference, ICT, Karlshruhe, Germany, 1996, p. 18/1.

[12] K. Schmid, D. Kaschmeiuder, Proceedings of the 31st International Annual Conference, ICT, Karlshruhe, June 2000, p. 110/1.

[13] J. Alster, S. Iyer, O. Sandus, in: S.N. Bulusu (Ed.), Chemistry and Physics of Energetic Materials, Kluwer Academic Publishers, Dortrecht, The Netherlands, 1990, p. 641.

[14] M.A. Hiskey, M.D. Coburn, M.A. Mitchell, J. Heterocyclic Chem. 29 (1992) 1855.

[15] A.R. Kartritzsky, D.J. Cundy, J. Chen, J. Heterocyclic Chem. 31 (1994) 271.

[16] T. Axenord, C. Watnick, H. Yazdekhasti, P.R. Dave, Tetrahedron Lett. 34 (1993) 6677.

[17] S. Zeeman, Thermochim. Acta 333 (1999) 257.

[18] Z. Jalovy, S. Zeman, M. Suceska, P. Vavra, K. Dudek, M. Rajic, J. Energetic. Mater. 19 (2001) 219.

[19] M. Suceska, M. Rajic, S. Zeman, Z. Jalovy, J. Energetic. Mater. 19 (2001) 259.

[20] M.A. Dewey, R.J. Blau, Dan W. Doll, K.E. Lee, P.C. Braithwaite, Melt/pour explosives containing TNAZ, in: Proceedings of the Insensitive Munitions and Energetic Materials Technology Symposium, Orlando, FL, March 10–13, 2003.

[21] T. Axenord, C. Watnick, H. Yazdekhasti, P.P. Dave, J. Org. Chem. 60 (1995) 1959–1964.

[22] N. Sikdar, A. Singh, A.K. Sikdar, Improved synthesis of an energetic material 1,3,3-trinitroazetidine (TNAZ) exploiting 2-iodoxy benzoic acid as an oxidizing agent, Indian J. Chem., Section B, in press.

[23] J. Zhang, Ch. Zhu, X. Gong, H. Xiao, Wuli Huaxue Xuebao 13 (1997) 612.

[24] J.C. Oxley, J. Smith, W. Zheng, E. Rogers, M. Coburn, J. Phys. Chem. A 101 (1997) 4375.

[25] C.P. Constantinou, C. Pereira, M.M. Chaudhari, Propellants, Explosives, Pyrotechnics 20 (1995) 200.

[26] L. Jinshan, X. Heming, D. Haishan, Propellants, Explosives, Pyrotechics 25 (2000) 26.